Slow Cellular Dynamics in MDCK and R5 Cells Monitored by Time-Lapse Atomic Force Microscopy

Cora-Ann Schoenenberger* and Jan H. Hoh‡

*Maurice E. Müller Institute for Microscopic Structural Biology, Biozentrum, University of Basel, CH-4056 Basel, Switzerland, and ‡Department of Physiology, School of Medicine, Johns Hopkins University, Baltimore, Maryland 21205 USA

ABSTRACT We have examined dynamic events that occur on a time scale of minutes in an epithelial monolayer of Madine-Darby Canine Kidney (MDCK) cells and in *ras*-transformed MDCK cells by atomic force microscopy (AFM). Cells were imaged under physiological conditions, and time-lapse movies representing ~60 s real time per frame were assembled. In normal MDCK cells, two types of protrusions in the apical plasma membrane exhibit dynamic behavior. First, smooth bulges formed transiently over the time scale of minutes to tens of minutes. Second, spike-like protrusions appear initially as bulges, extend well above the apical surface and, finally, seem to detach. R5, an oncogenic transformant derived from MDCK cells, grows very flat on glass. During AFM imaging, these cells sometimes round up and detach from the substrate. In light microscopic observations of parallel preparations, cells rarely detach, suggesting that this is an active response of these cells to irritation by the AFM tip. R5 cells often extend processes that are supported by actin stress fibers. During imaging with the AFM, these processes withdraw at a rate of 1–5 μm/min, similar to that observed by light microscopy. During the withdrawal, movement of the stress fibers can be clearly seen. In the flat periphery of these cells, the transport of intracellular particles along cytoskeletal elements was seen. In addition, we have observed two types of wave-like movements through the cell, which appear to be an organized rearrangement of cytoplasm. One type of wave moves radially out from center of the cell while the other moves circularly along the cell periphery.

INTRODUCTION

We have recently described the morphology of Madine-Darby Canine Kidney (MDCK) cells and a transformant (R5) derived from MDCK by retroviral infection with the K-*ras* oncogene, by atomic force microscopy (AFM; Binnig et al., 1986) (Hoh and Schoenenberger, 1994). The apical plasma membrane of MDCK cells is very soft, with a stiffness that is much lower than the spring constant for the AFM cantilevers used ($k_{cant.}$ = 0.06 N/m). This results in a deformation of the membrane around more rigid intracellular structures and allows a number of them, including the nucleus, actin fibers, and vesicles to be visualized (Henderson et al., 1992; Chang et al., 1993; Fritz et al., 1994; Hoh and Schoenenberger, 1994; for a review, see Henderson, 1994). In addition, we have described two novel structures called spikes and bulges, for which no corresponding structures have been identified in light or electron microscopy. The unique contrast mechanism of the AFM now allows the dynamic behavior of these intracellular structures to be examined directly. In this report, we have produced time-lapse movies from AFM data that reveal extensive movement in both MDCK and R5 cells. For the R5 cells, the movies show the dynamics of stress fibers that is consistent with the movement of cytoskeleton previously observed (Henderson et al., 1992; Chang et al., 1993) and a wave-like rearrangement of cytoplasm similar to that reported by Kasas and co-workers (1993). In addition, the motion of intracellular particles along cytoskeletal elements is monitored. In MDCK cells, we see both spikes and bulges at the apical surface move.

Received for publication 7 March 1994 and in final form 17 May 1994.

© 1994 by the Biophysical Society

0006-3495/94/08/929/08 $2.00

MATERIALS AND METHODS

Cell culture

MDCK strain II epithelial cells (low transmonolayer resistance; Matlin and Simons, 1983) were subcloned by limiting dilution and a clone was chosen on the basis of its cuboidal morphology, growth rate, ability to form domes, and transepithelial resistance. The R5-transformed cell line was generated by retroviral infection of the MDCK subclone with the viral Kirsten *ras* oncogene (Schoenenberger et al., 1991). For routine culture on plastic substrates (Falcon), MDCK and R5 cell lines were grown in Eagle's minimal essential medium supplemented with Earle's salts (GIBCO BRL, Basel), 5% fetal bovine serum, 2 mM L-glutamine, and 10 mM HEPES, pH 7.3 at 37°C in a 95% air/5% CO_2-humidified incubator. Confluent cells were released from the plastic using trypsin-EDTA (GIBCO BRL) and passaged at appropriate dilutions. Routine and experimental cultures were fed with fresh medium every other day.

Sample preparation for AFM imaging

To prepare samples for imaging, round glass coverslips (12 mm) were glued onto magnetic steel stubs (needed for mounting samples in the AFM), autoclaved, and placed in tissue culture dishes. Confluent MDCK cells grown on plastic were trypsinized, counted, and adjusted to 6×10^5 cells/ml. 100 μl of the cell suspension was plated on a mounted coverslip and spread to cover the entire surface. Cells were allowed to attach for several hours at 37°C in 95% air/5% CO_2 before adding medium to the tissue culture dish. On day 4 after plating, monolayers of MDCK cells had nearly reached saturation density and were used for imaging. R5 cells were plated at low densities (<10^4 cells/coverslip) and imaged 2 days after plating. All imaging was performed with cells at passages <15.

Atomic force microscopy

A Nanoscope III atomic force microscope (Digital Instruments Inc., Santa Barbara, CA) was used for all AFM imaging. This microscope was equipped with a large-area scanner (J type) with a maximum *xy* scan range of 160 μm × 160 μm and a *z* range of 5 μm. Cantilevers were standard microfabricated (Albrecht et al., 1990) V shaped, 200 μm long with 40 μm wide legs, silicon nitride Nanoprobes (Digital Instruments). A spring constant of 0.06 N/m, determined by the method of Cleveland et al. (1993), was used to estimate

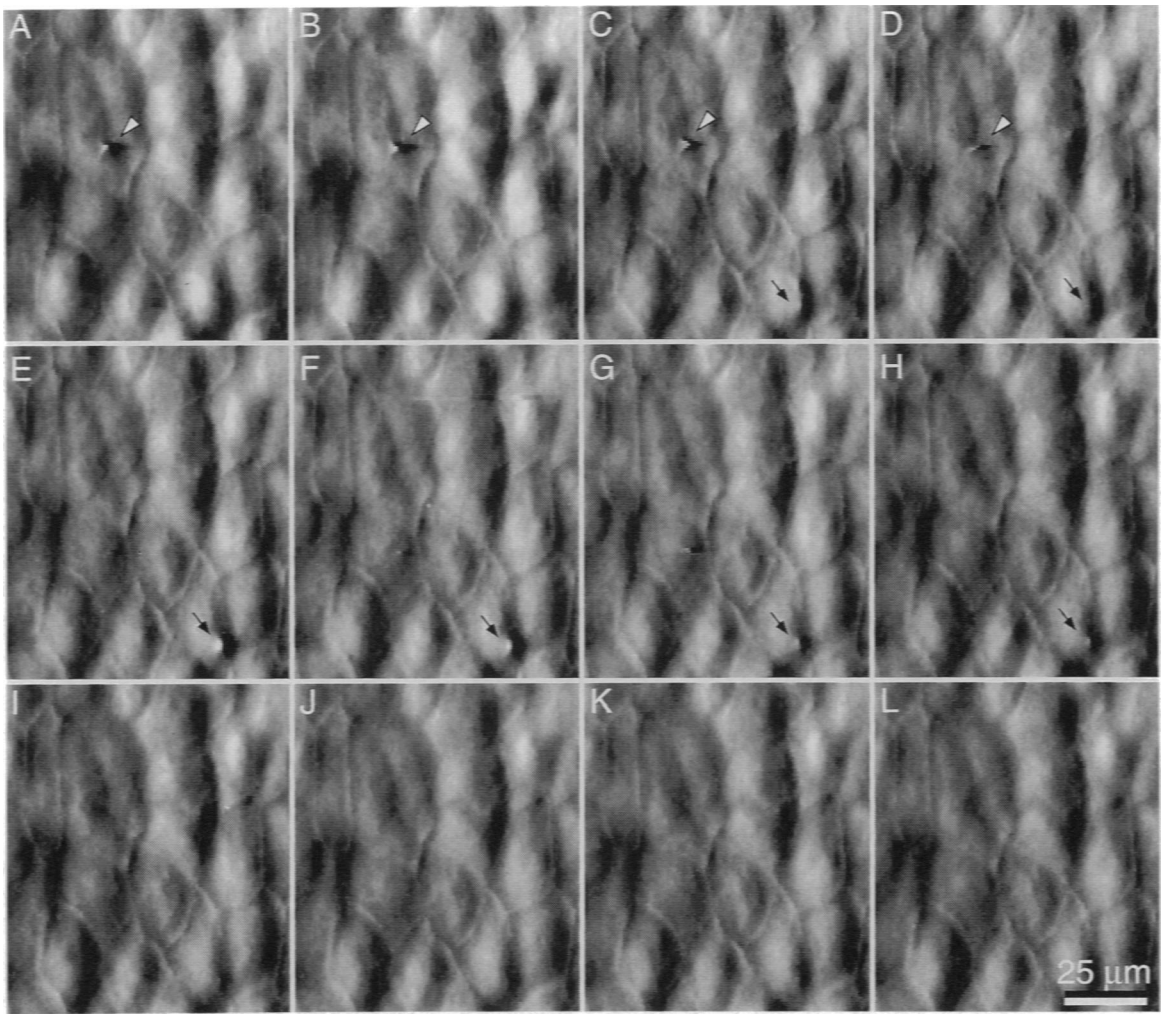

FIGURE 1 Time-lapse AFM series from an MDCK monolayer showing a transient bulge in the apical membrane. Each frame is taken ~80 s apart. A pair of bulges (*black arrow*) appear in frame *C* and recede in *D*. The lower of the bulges then again pushes against the apical plasma membrane in *E* before receding gradually in *E–I*. Frame *A* shows a spike that was present at the onset of imaging (*white arrow*). This spike disappears from one line scan to the next during the acquisition of the image in frame *D*, resulting in a half spike (slow scan direction is up). In the next image the spike is no longer visible.

imaging forces. A standard fluid cell was used without the o-ring, similar to the "trapped drop" approach used in the first AFM imaging in liquids (Drake et al., 1989). Imaging of cells was performed in phosphate-buffered saline (PBS, 140 mM NaCl, 10 mM Na_2HPO_4, pH 7.2) containing 1 mM $CaCl_2$ and 0.5 mM $MgCl_2$. To compensate for evaporation from the unsealed fluid cell, buffer was exchanged at regular intervals. Microscope parameters were similar to those previously described (Hoh et al., 1993). The most critical imaging parameters were imaging force and scan rate. Scan rates were kept at 50–500 μm/s, and the imaging force was maintained just high enough to achieve good contrast (typically ~2 nN; Hoh and Schoenenberger, 1994). Error signal images were collected by monitoring the deflection signal with the gains set as high as possible without the feedback loop oscillating (Hoh and Hansma, 1992; Putman et al., 1992). This produces an effect similar to a high pass filter in which quantitative height information is lost. Constant force images with the true height (*z* piezo position) were collected simultaneously and used for all height and volume measurements; however, only error signal images are shown. For a given series (except Fig. 1), images were only collected in one slow scan direction by using the frame up/down function once an image was complete. All images are raw data from the AFM with no processing.

Image display and time-lapse series

Series of AFM images were acquired at time intervals of 50–100 s, roughly the time to complete a single scan. To produce time-lapse movies, images were imported into the NIH *Image* program. Sequential images representing the same slow scan direction (up or down) were assembled into a movie using *Image* and played back at ~1000x real time, except in Fig. 1, where both up and down images were included. Movies were used to discern structures that moved on the time scale of imaging. Rates were determined using real-time calibrated sequences of images. Movies for Figs. 1, 3, 5, and 6 are available as a supplement from the Biophysical Journal FTP site. These can be viewed using NIH *Image* on Macintosh computers.

Light microscopy

R5 cells were plated and grown on glass coverslips under conditions corresponding to R5 specimens prepared for AFM imaging. The coverslips were mounted upside down on a glass slide with a spacer, thereby forming a chamber. The chamber was partially sealed with paraffin, replenished with medium, and mounted on a Zeiss Axiophot microscope (Carl Zeiss, Oberkochen, Germany). Loss of medium during imaging was compensated by perfusion of medium into the chamber. R5 cells were observed by video-enhanced differential interference contrast (DIC) microscopy at room temperature. Video films were recorded with an MXRi-intensified video camera at low-level illumination, processed with a DVS-3000 Hamamatsu image processor, and stored on a Sharp video recorder. Still-frames were captured from video tapes by the Image-1 image processing system.

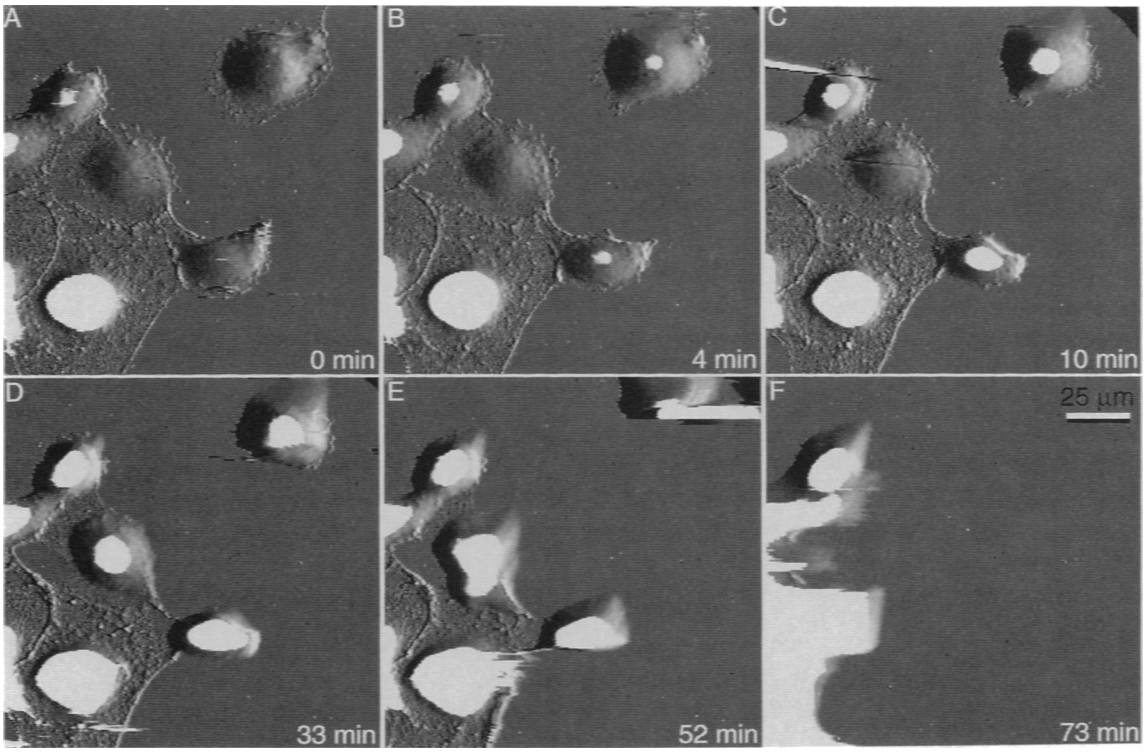

FIGURE 2 Rounding up of R5 cells in response to AFM imaging. (*A*) Initially, AFM images of R5 cells exhibit a morphology similar to that seen by light microscopy. (*B–F*) Cells begin to round up and detach from the surface. The increase of the white centers of the cells representing areas that are out of the *z* range of the scanner and cantilever, and the contribution of tip shape to the edges of the cells, indicate the rounding up cells increase in height.

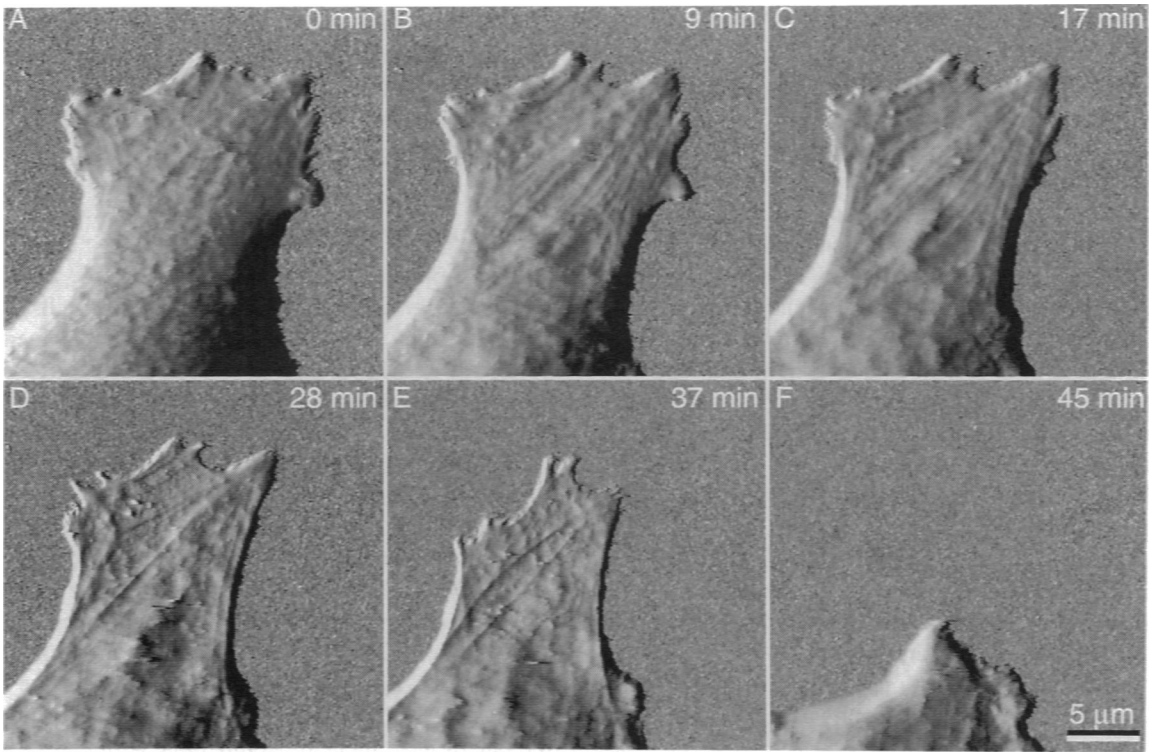

FIGURE 3 Time-lapse AFM series of process movement in an R5 cell. (*A–F*) R5 cells have extensive processes that withdraw toward the cell body during AFM imaging at a rate of 1–5 μm/min. As the process begins to move, stress fibers become apparent (*B*). Although the plasma membrane is very soft and actually deformed around the fibers, the fibers themselves are not displaced laterally.

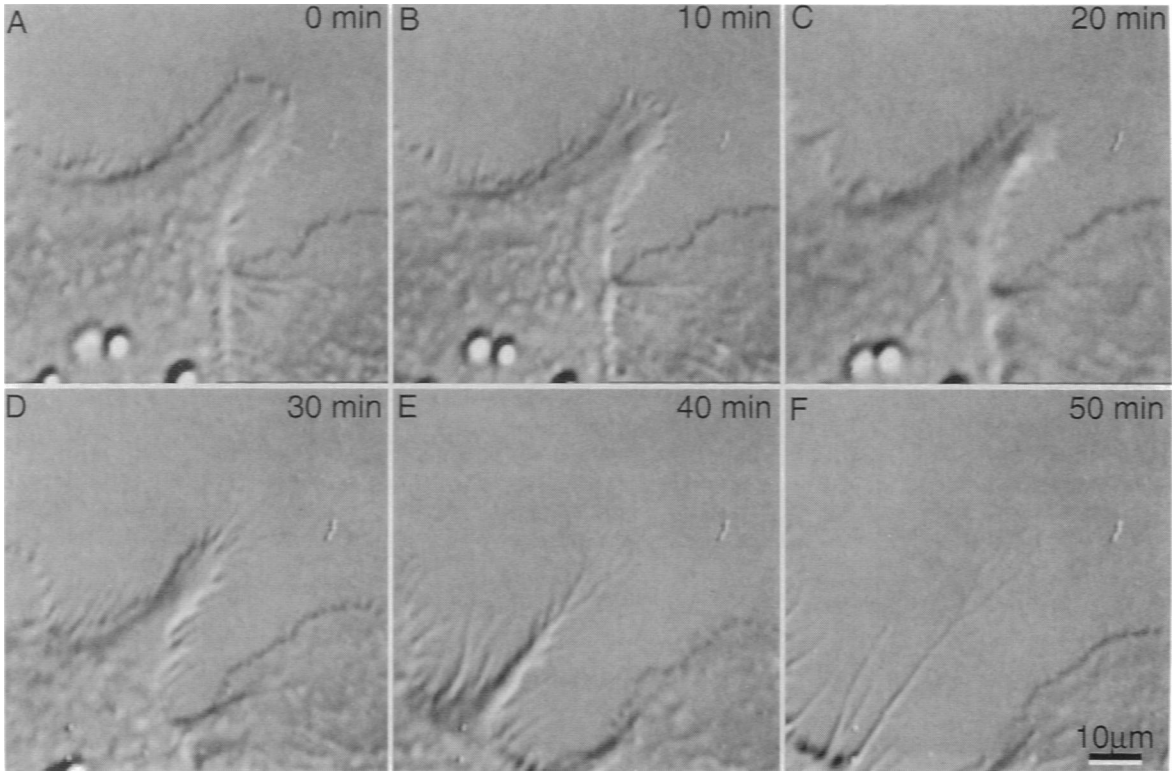

FIGURE 4 Differential interference contrast microscopy of process movement in R5 cells. *A–F* illustrate that the morphology and kinetics of process withdrawal are similar to the AFM series (Fig. 3).

RESULTS

Dynamic events at the apical membrane of MDCK cells

We have previously reported on two types of surface protrusions at the apical membrane of MDCK monolayers, bulges and spikes (Hoh and Schoenenberger, 1994). Both appear to represent relatively rigid subapical structures. A bulge is a smooth undulation in the surface, whereas spikes extend well above the surrounding membrane and are swept along the scan direction by the AFM tip. As shown in Fig. 1, both types of protrusions show dynamic behavior on the scale of tens of minutes. The submembrane structure that gives rise to the bulges pushes into the plasma membrane and then gradually retracts. Spikes, on the other hand, are often present at the onset of imaging or appear slowly, and then completely disappear within a single frame (Fig. 1 *D*). The sudden disappearance of spikes represents a very fast event, occurring within the time frame of one or a few scan lines in x, with each line being acquired in ~200 ms. Spikes will sometimes appear to move across the surface in the fast scan (x) direction. However, comparison of trace and retrace images shows that the apex of the spike is displaced in the fast scan direction with respect to a center position, indicating that it is simply bending further on each scan (data not shown).

Fixation of the MDCK monolayer with glutaraldehyde results in a rapid stiffening of the monolayer as previously described (Hoh and Schoenenberger, 1994). In addition, fixation eliminates all motion in the cells and time-lapse series of fixed monolayers show no movement over extended time periods. The cells also died when the fluid was not replenished in the fluid cell, because evaporation from the unsealed fluid cell lead to a detrimental increase in salt concentration. In this case, cellular motions no longer occurred (data not shown).

Movement in R5 cells

Unlike normal MDCK cells, the oncogenic derivative R5 does not form distinct islands of polarized cells, but rather spread out and extend numerous processes (Schoenenberger et al., 1991). AFM imaging of these cells at sub-confluency reveals this typical morphology (Fig. 2 *A*). Although these cells are generally stable for hours, in some of our experiments individual R5 cells round up and detach from the surface over tens of minutes. Such a series is shown in Fig. 2. Occasionally, one or two images were sufficient to induce cell detachment tens of minutes later. Light microscopy of R5 cells only rarely shows cells detach, which suggests that the rounding up is stimulated by the AFM tip.

At higher magnification, individual processes from R5 cells imaged with the AFM withdraw toward the cell body at a rate of 1–5 μm/min (Fig. 3). The cell morphology and the rate of movement are comparable with that seen by light microscopy in parallel preparations (Fig. 4). During the retraction, the stress fibers and their dynamic changes can be visualized by AFM. Notably, there is no significant lateral

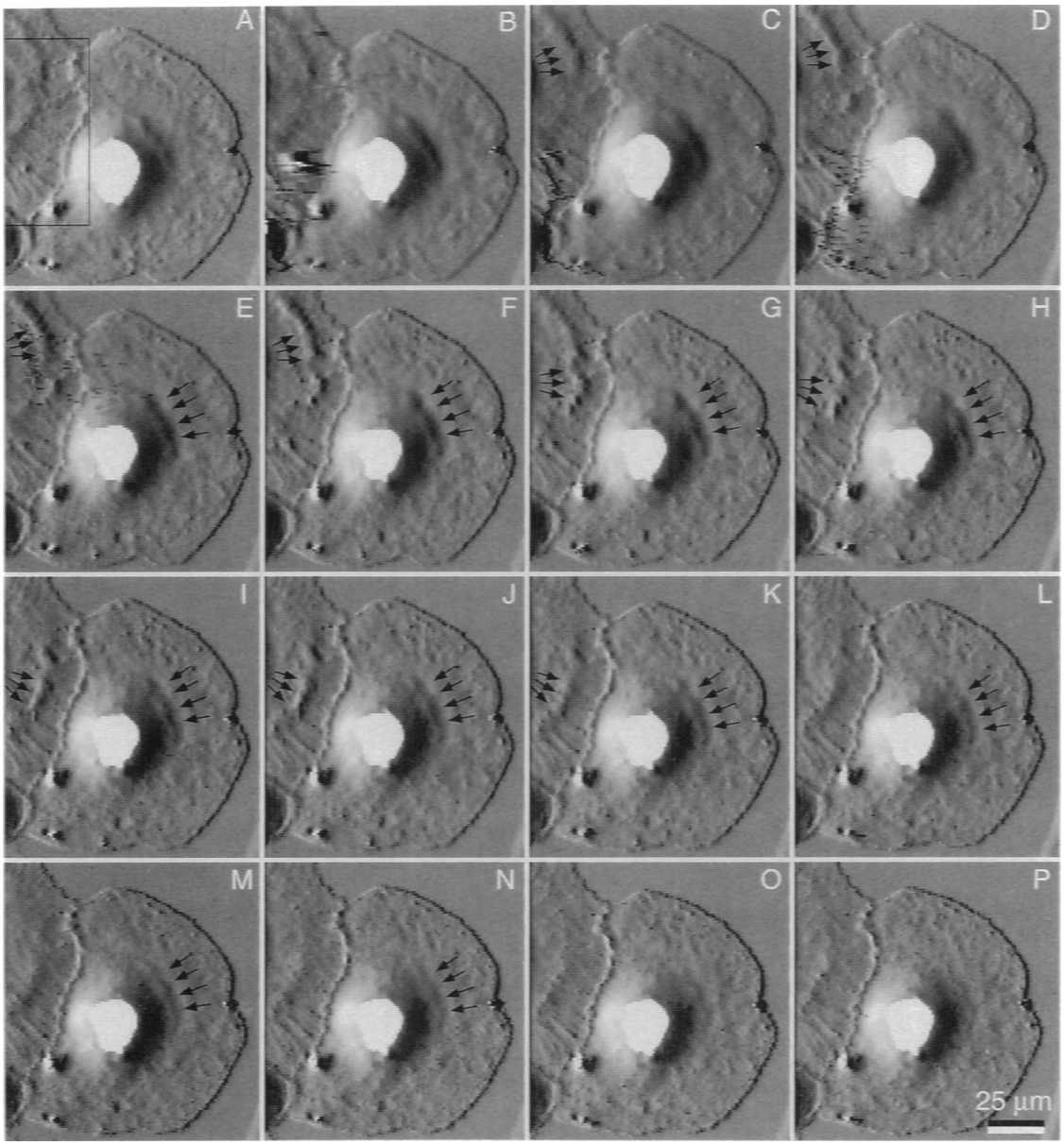

FIGURE 5 Time-lapse AFM series of two adjacent R5 cells showing wave-like rearrangement of cytoplasm through the flat regions of these cells. One wave (*three arrows*) begins in frame *C*, moves through the left cell parallel to the cell boundary at a rate of ~3 μm/min (*C–L*). A second wave (*four arrows*) propagates radially from the nucleus (*white area*), similar to a ripple in water, at a rate of ~0.2 μm/min. The time between each frame is ~90 s, and the slow scan direction is up. The box in *A* shows the region magnified in Fig. 6.

displacement (in the fast scan direction) of the stress fibers, indicating that they are rigid relative to the lateral forces exerted by the tip.

Occasionally, we have observed what seems to be a rearrangement of cytoplasm in R5 cells. This rearrangement occurs in a wave-like fashion. There are two types of waves, one that propagates radially out from the nucleus and one that propagates circularly around the edge of the cell. Both types of waves are shown in Fig. 5. There, the circular wave has an estimated volume of 100 μm^3, as calculated from the part that extends above the surrounding plasma membrane (using height data collected in parallel with the error signal images shown in Fig. 5). It moves parallel to the cell boundary, across cytoskeletal elements that extend towards the nucleus, at a rate of ~3 μm/min. In contrast, the radial wave propagates away from the nucleus at a rate of ~0.2 μm/min. Because this wave is much shallower, it is difficult to determine the plane of the surrounding plasma membrane and estimate a volume. However, it is significantly less than for the circular wave.

In the flat periphery of R5 cells, many particles that appear to be intracellular vesicles can be seen. Time-lapse movies show that some of these vesicles move relative to other structures within the cell. Fig. 6 shows several vesicles moving along the fibrous structures inside the cell at a rate of ~0.1 μm/min. We interpret these to be vesicles being

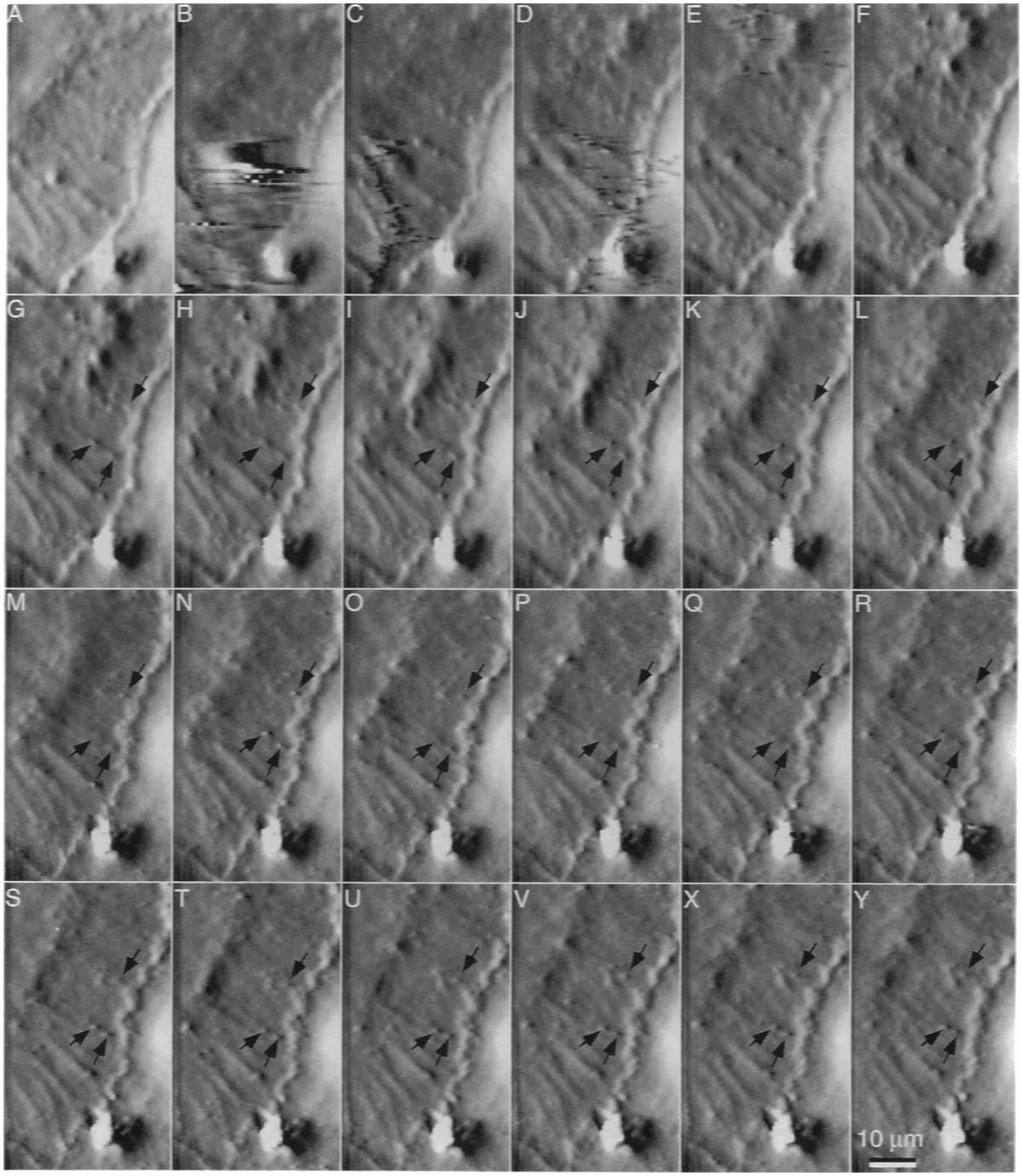

FIGURE 6 Time-lapse AFM series from the flat periphery of an R5 cell. Particles move along cytoskeletal elements that run perpendicular to the periphery of the cell. The single arrow points to a vesicle moving from the edge of the cell toward the center. The pair of arrows indicates two different vesicles that are moving toward each other. For these particles, the rate of movement is ~0.1 μm/min. Series is from the boxed region in Fig. 5 *A*.

transported along cytoskeletal elements. The fact that they can withstand the lateral forces encountered during imaging suggests that the association of the vesicle with the cytoskeletal tracks is fairly strong.

DISCUSSION

Time-lapse atomic force microscopy

The ability of the AFM to directly visualize relatively rigid structures within a cell, in effect staining the cell based on mechanical properties, has revealed a variety of intracellular structures (Henderson et al., 1992; Chang et al., 1993; Kasas et al., 1993; Hoh and Schoenenberger, 1994). The analysis of sequential images has shown that the position of these structures can change, indicating that cellular dynamics can be examined by AFM. Although in principle it is possible to detect structural changes by comparing individual sequential images, in practice the complexity of the features in many images makes it very difficult. To circumvent this problem, we have time-lapsed series of AFM images of MDCK and

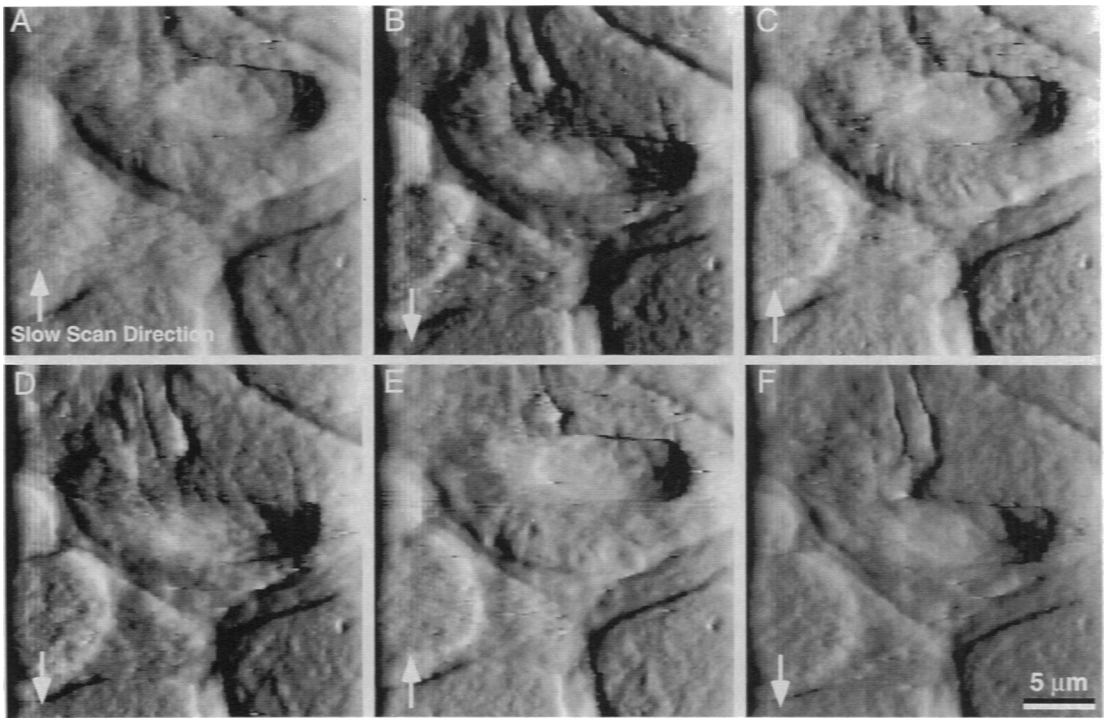

FIGURE 7 Displacement of cellular structures in the slow scan direction. (*A–F*) Sequence of alternating up and down scans shows that the nucleus in this MDCK cell is displaced along the slow scan direction.

R5 cells and produced movies. This presentation of AFM data was first used by Drake et al. (1989) to examine fibrin assembly, by Hörber and colleagues (1992) to investigate cells infected with pox virus, and by Hillner et al. (1992) to show atomic scale growth of calcite. The time-lapse display takes advantage of the human eye's sensitivity to motion to identify structures that move or change shape, and was critical to identifying the dynamics described in this report.

Rates of movement

The average image acquisition time for the results presented here is ~60 s. This is a relatively long time compared with many cellular events, and as a result fast events will be filtered out of the movies. However, single lines are often scanned at <200 ms, and the response time of the cantilever, which is limited by its resonant frequency in solution (Butt et al., 1992), is <1 ms at any one point on the surface. Therefore, if the scanned area is sufficiently small, events much faster than the ones described here could be followed. The disappearance of spikes, for instance, occurs from one scan line to the next (see Fig. 1 *D*) and, thus, is a relatively fast event that occurs on the order of several hundred milliseconds.

The rate of retraction for the R5 processes we have measured in the AFM is ~1–5 μm/min, comparable with that seen by light microscopy. This suggests that the dynamics of the system are not seriously perturbed by the interaction with the AFM tip. In contrast, the vesicle movement we have detected is significantly slower than measurements typically reported by light microscopy, which are often on the order of micrometers per second (Rebhun, 1972). This can be explained by the effect described above, in which fast moving vesicles are filtered out by the slow scan rate, thereby selectively imaging a class of slow moving vesicles. Alternatively, some vesicles may be knocked off the cytoskeletal tracks, leaving only a subset of vesicles that associate tightly during transport.

Moving structures

A significant component of the contrast in AFM images of living cells depends on the compliance of the plasma membrane, which allows it to deform around more rigid intracellular structures. This unique contrast mechanism has allowed us to identify two structures in MDCK cells, spikes and bulges, for which counterparts have not been identified by other microscopic techniques. In this report, we show that spikes and bulges exhibit dynamic behavior. However, the nature of these structures remains unknown. The wave-like movements in R5 cells are also of unknown origin. The wave that emanates radially from the nucleus appears to be similar to that described in lung carcinoma cells (Kasas et al., 1993). In addition, we have seen a wave that propagates parallel to the cell periphery. That the two waves move essentially perpendicular to each other indicates that they are not a passive response to the AFM tip. In addition, the slow scan in this series is up, and neither of the waves moves in that direction. These waves are reminiscent of calcium waves that can be induced in cultured cells (Berridge and Irvine, 1989; Lechleiter et al., 1991). However, the waves we observe in R5 cells cannot simply represent a change in ion concentration, because this would provide no basis for contrast in the AFM. Rather, the wave must represent a rearrangement of structures within the cytoplasm or an organization of

cytoplasm into a region with mechanical properties different from unorganized cytoplasm.

Given the ability of the AFM tip to displace structures, care must be taken to understand what is authentic cellular movement and what is displacement by the tip (tip-*induced* movements are discussed below). The most distinguishing feature of displacement is that it depends on the scan direction. An example is the apparent lateral movement of spikes in the fast scan direction. However, we have also seen displacement of intracellular structures in the slow scan direction. Fig. 7 shows the nucleus of an MDCK cell being displaced. The tip apparently nudges the nucleus in the slow scan direction on each scan line.

Cell irritation by the AFM tip

We have previously shown that the apical membrane of MDCK cells is soft relative to the cantilevers used and deforms up to 500 nm when 1 nN force is applied to the cell with a pyramidal tip, indicating that there is a significant indentation of the membrane under standard imaging conditions (Hoh and Schoenenberger, 1994). Furthermore, it is well documented that stimulating cells by poking them with needles, or other forms of physical stimulus, induces structural and physiological changes (e.g., Charles et al., 1991; McNeil, 1993). Similarly, it has also been shown that the AFM tip can induce the activation blood platelets (Fritz et al., 1993). One must therefore consider the possibility that the movements we see are similarly induced by the AFM tip. In MDCK cells, we do not see any responses that can be attributed to stimulation by the AFM tip. In contrast, the propensity of the R5 cells to round up during imaging appears to result from stimulation by the tip. Accordingly, we did not observe any cells detach from the substrate by light microscopy. A similar loss of contact with the substrate after prolonged AFM imaging was described by Papura and colleagues (1992). Although these responses to the tip may limit the applications of the AFM for imaging living cells, they also indicate that the AFM can become a tool for applying stimuli and, for example, mapping mechanical signal transduction systems.

We gratefully acknowledge Markus Dürrenberger and Robert Häring for advice on video light microscopy. We thank Ueli Aebi, Andreas Engel, and Paul Hansma for their generous support, Jason Cleveland, Monika Fritz, Helmut Knapp, and Frank Schabert for helpful discussions, and Manfred Radmacher for a critical reading of the manuscript.

This research was supported by a postdoctoral fellowship from the Human Frontier Science Program Organization (to J. H. Hoh, LT-438/92), a junior scientist award from the Paul Blümel Foundation (to C. A. Schoenenberger), and the M. E. Müller Foundation.

REFERENCES

Albrecht, T. R., S. Akamine, T. E. Carver, and C. F. Quate. 1990. Microfabrication of cantilever styli for the atomic force microscope. *J. Vac. Sci. Technol. A.* 8:3386–3396.

Berridge, M. J., and R. F. Irvine. 1989. Inositol phosphates and cell signalling. *Nature.* 341:197–205.

Binnig, G., C. F. Quate, and C. Gerber. 1986. Atomic force microscope. *Phys. Rev. Lett.* 56:930–933.

Butt, H.-J., P. Siedle, K. Seifert, K. Fendler, T. Seeger, E. Bamberg, A. L. Weisenhorn, and A. Engel, Scan speed limit in atomic force microscopy. 1993. *J. Microsc.* 169:75–84.

Chang, L., T. Kious, M. Yorgancioglu, D. Keller, and J. Pfeiffer, J. 1993. Cytoskeleton of living, unstained cells imaged by scanning force microscopy. *Biophys. J.* 64:1282–1286.

Charles, A. C., J. E. Merrill, E. R. Dirksen, and M. Sanderson. 1991. Intercellular signaling in glial cells: calcium waves and oscillations in response to mechanical stimulation and glutamate. *Neuron.* 6:983–992.

Cleveland, J. P., S. Manne, D. Bocek, and P. K. Hansma. 1993. A nondestructive method for determining the spring constant of cantilevers for scanning force microscopy. *Rev. Sci. Instr.* 64:403–405.

Drake, B., C. B. Prater, A. L. Weisenhorn, S. A. C. Gould, T. R. Albrecht, C. F. Quate, D. S. Cannell, H. G. Hansma, and P. K. Hansma. 1989. Imaging crystals, polymers, and processes in water with the atomic force microscope. *Science.* 243:1586–1589.

Fritz, M., M. Radmacher, and H. E. Gaub. 1993. In vitro activation of human platelets triggered and probed by atomic force microscopy. *Exp. Cell Res.* 205:187–190.

Fritz, M., M. Radmacher, N. Peterson, and H. E. Gaub. 1994. Visualization of intracellular structures via force modulation and chemical degradation. *J. Vac. Sci. Technol. B.* In press.

Henderson, E., P. G. Haydon, and D. S. Sakaguchi. 1992. Actin filament dynamics in living glial cells imaged by atomic force microscopy. *Science.* 257:1944–1946.

Henderson, E. R. 1994. Imaging living cells by atomic force microscopy. *Prog. Surf. Sci.* 46:39–60.

Hillner, P. E., S. Manne, A. J. Gratz, and P. K. Hansma. 1992. AFM images of dissolution and growth on a calcite crystal. *Ultramicrosc.* 42: 1387–1393.

Hoh, J. H., and P. K. Hansma. 1992. Atomic force microscopy for high resolution imaging in cell biology. *Trends Cell Biol.* 2:208–213.

Hoh, J. H., and C.-A. Schoenenberger. 1994. Surface morphology and mechanical properties of MDCK monolayers by atomic force microscopy. *J. Cell Sci.* 107:1105–1114.

Hoh, J. H., G. E. Sosinsky, J.-P. Revel, and P. K. Hansma. 1993. Structure of the extracellular surface of the gap junction by atomic force microscopy. *Biophys. J.* 65:149–163.

Hörber, J. K. H., W. Haberle, F. Ohnesorge, and G. Binnig. 1992. Investigation of living cells in the nanometer regime with the scanning force microscope. *Scanning Microsc.* 6:919–930.

Kasas, S., V. Gotzos, and M. R. Celio. 1993. Observation of living cells using the atomic force microscope. *Biophys. J.* 64:539–544.

Lechleiter, J., S. Girard, E. Peralta, and D. Clapham. 1991. Spiral calcium wave propagation and annihilation in *Xenopus laevis* oocytes. *Science.* 252:123–126.

Matlin, K. S., and K. Simons. 1983. Reduced temperature prevents transfer of a membrane glycoprotein to the cell surface. *Cell.* 34:233–243.

McNeil, P. L. 1993. Cellular and molecular adaptations to injurious mechanical stress. *Trends Cell Biol.* 3:302–307.

Parpura, V., P. G. Haydon, and E. Henderson. 1993. Three-dimensional imaging of living neurons and glia with the atomic force microscope. *J. Cell Sci.* 104:427–432.

Putman, C. A. J., K. O. van der Werf, B. G. de Grooth, N. F. van Hulst, J. Greve, and P. K. Hansma. 1992. A new imaging mode in atomic force microscopy based on the error signal. *Proc. Soc. Photo-Opt. Instr. Eng.* 1639:198–204.

Rebhun, L. I. 1972. Polarized intracellular particle transport: saltatory movements and cytoplasmic streaming. *Int. Rev. Cytol.* 32:93–131.

Schoenenberger, C.-A., A. Zuk, D. M. Kendall, and K. S. Matlin. 1991. Multilayering and loss of apical polarity in MDCK cells transformed with viral K-*ras*. J. Cell Biol. *J. Cell Biol.* 112:873–889.